International Research Journal of Engineering and Technology (IRJET) e-ISSN: 2395-0056
Volume: 07 Issue: 07 | July 2020 www.irjet.net p-ISSN: 2395-0072

STUDY ON GENERATION OF URBAN HEAT ISLAND WITH INCREASING URBAN SPRAWL IN GAUTAM BUDDHA NAGAR (NOIDA) UTTAR PRADESH, INDIA

Abhijeet Singh[1], Ajeetam Krishna[2], Pragati Singh[3], Dr. Rajesh Kumar Upadhyay[4]

[1]*PG student, Agriculture Resources Division, Remote Sensing Applications Centre Uttar Pradesh*
[2]*PG student, Agriculture Resources Division, Remote Sensing Applications Centre Uttar Pradesh*
[3] *Project Scientist, Agriculture Resources Division, Remote Sensing Applications Centre Uttar Pradesh*
[4] *Scientist-SE and Head, Agriculture Resources Division, Remote Sensing Applications Centre Uttar Pradesh*

ABSTRACT- *Land surface temperature (LST) is an important factor in many fields, such as study of global climate change, urban sprawl, geo-biophysical and also a crucial input for climate models. LANDSAT 8, the latest satellite from the LANDSAT series, has made it possible to study land processes using remote sensing. In this study an attempt has been made to estimate LST with respect to urban sprawl in Gautam Buddha Nagar district of Uttar Pradesh India, using LANDSAT-8 – Operational Land Imager & Thermal Infrared Sensor (OLI & TIRS) satellite data with spatial resolution 30m and 100m. The variability of LSTs has been retrieved using Brightness Temperature (BT) values and Land Surface Emissivity values (LSE- which has been calculated using Normalized Difference Vegetation Index NDVI). The present study shows that continuous increase in urban sprawl results increase of land surface temperature from 2014 to 2018 over Gautam Buddha Nagar district of Uttar Pradesh, India.*

Keywords: Land Surface Temperature (LST), Land Surface Emissivity (LSE), Normalized Difference Vegetation Index (NDVI), Operational Land Imager & Thermal Infrared Sensor (OLI & TIRS), Urban Heat Island (UHI), Urban Sprawl.

1. INTRODUCTION

Land Surface Temperature (LST) is the skin temperature of the earth crust which can directly measured by the remote sensing satellite (Jeevalakshmi, Reddy, & Manikiam, 2017).Global urbanization has drastically reshaped the panorama, which has vital climatic indications throughout all scales because of the simultaneous change of natural land cover and advent of urban materials i.e. Anthropogenic surfaces. Identification and characterization of Urban Heat Island is typically based on LST that range spatially, due to the non-homogeneity of land surface cover and other different atmospheric factors (Joshi & Bhatt, 2012).Ground surveys would allow a highly accurate Land Use Land Cover classification, but they are time-consuming and costly, which highlights remote sensing clear and preferred substitute. Medium spatial resolution data, such as LANDSAT-8 is fit for land cover or vegetation mapping at regional local scale. LANDSAT-8 carries two sensors, i.e., Operational Land Imager (OLI) and the Thermal Infrared Sensor (TIRS). OLI collects data at a 30m spatial resolution with eight bands which is placed in the visible and near-infrared region and the shortwave infrared regions of the electromagnetic spectrum, and an additional panchromatic band of 15m spatial resolution. TIRS senses the TIR radiance at a spatial resolution of 100m using two bands located in the atmospheric window between 10 and 12 µm(Jimenez-Munoz J.-C. , Sobrino, Skokovic, Mattar, & Cristóbal Rosselló, 2014)(Tomlinson, Chapman, Thornes, & Baker, 2011).

Diverse techniques have been evolved to estimate LST for Urban Heat analysis, Climatology, Meteorology and Land Cover Dynamic monitoring with the use of brightness temperature (Joshi & Bhatt, 2012).The technique presented in this paper is used for estimating the LST of a given LANDSAT-8 image with the input of the red band (0.64–0.67 µm), near infrared band (NIR) (0.85–0.88 µm), and thermal infrared band10 (TIR) (10.60– 11.19µm) and the urban sprawl by digitizing.

2. STUDY AREA

2.1. Gautam Buddha Nagar

Gautam Buddha Nagar district is situated in the Doab of Ganga and Yamuna rivers between the parallels of 28º 6' to 28º 40' North and 77º 17' to 77º 42' East meridians. It is bounded in the North by district Ghaziabad and in the South by district Aligarh. In the east lies district Bulandshahr (Chen, 2002)(Chen, 2002)(Bonafoni & Keeratikasikorn, 2018). In the west river Yamuna forms natural boundary with the state of Delhi and Faridabad district of Haryana state. The district is vertically stretched from North to South rather than East to West. The total area of the district is 1282 sqkms.

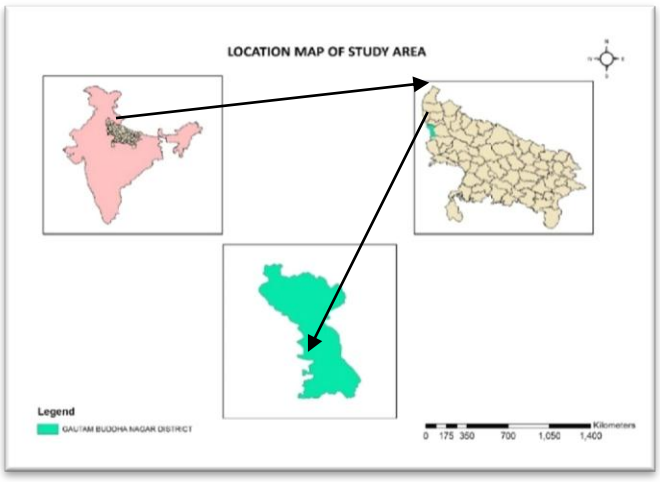

FIGURE 1: location map of Gautam Buddha Nagar district

3. DATA AND METHODOLOGY

The multispectral remote sensing images of Gautam Buddha Nagar district from 2014 to 2018 were collected from USGS. Landsat 8 satellite provide16 day's temporal resolution data. Band properties of Landsat-8 are as given in Table1. Satellite data over Gautam Buddha Nagar district of from 2014 to 2018 (day time, level-1G product, path/row 146/40) have been used in this study. The study area consists of bare soil, vegetation cover, water, and built-up area.

[1] **TABLE 1:** Landsat 8 bands properties

SENSOR	BAND NUMBER	BAND NAME	WAVELENGTH (µm)	RESOLUTION (M)
OLI	1	COASTAL	0.43 - 0.45	30
OLI	2	BLUE	0.45 - 0.51	30
OLI	3	GREEN	0.53 - 0.59	30
OLI	4	RED	0.63 - 0.67	30
OLI	5	NIR	0.85 - 0.88	30
OLI	6	SWIR 1	1.57 - 1.65	30
OLI	7	SWIR 2	2.11 - 2.29	30
OLI	8	PAN	0.50 - 0.68	15
OLI	9	CIRRUS	1.36 - 1.38	30
TIRS	10	TIRS 1	10.60 - 11.19	100
TIRS	11	TIRS 2	11.50 - 12.51	100

The LST of Landsat-8 satellite image has been retrieved by following the steps of Figure 1. In this study, the TIR band 10 is used to estimate brightness temperature and bands 4 and 5 is used for calculating the NDVI. The values of different variables have been taken from the Metadata file which is presented in Table 2.

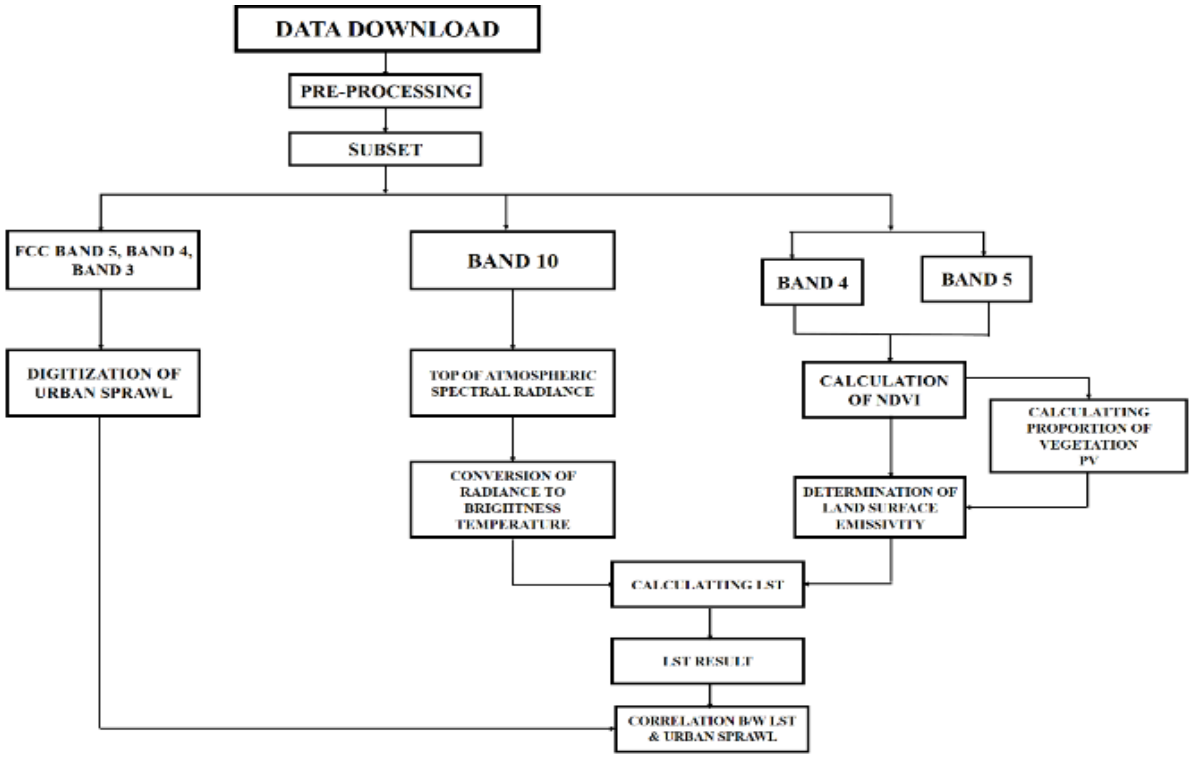

FIGURE 2: flow diagram of urban sprawl and lst retrieval

3.1. Step1:

The initial step of the calculation is the input of Band 10. After inputting band 10, in the background, the tool uses formulas for retrieving the top of atmospheric (TOA) spectral radiance L_λ.

$$L_\lambda = M_L * Q_{cal} + A_L - O_i \quad (1)$$

Where M_L represents the band-specific multiplicative rescaling factor, Q_{cal} is the Band 10 image, A_L is the band-specific additive rescaling factor, and O_i is the correction for Band 10 (Avdan & Jovanovska, 2016).

3.2. Step 2:

After the digital numbers (DNs) are converted to reflection, the TIRS band data needs to be converted from spectral radiance to brightness temperature (BT) using the thermal constants provided in the metadata file.

$$B_T = \frac{/K2}{\ln (k1 / L\lambda + 1)} - 273.15 \quad (2)$$

Where k_1 and K_2 stand for the band-specific thermal conversion constants obtained from the metadata. For acquiring the results in Celsius, the radiant temperatures revised through including the absolute zero (approx. −273.15°C) (Jeevalakshmi, Reddy, & Manikiam, 2017).

TABLE 2: metadata of the satellite images.

Variable	Description	Value
M_L	Rescaling factor, Band 10	0.000342
A_L		0.1
k_1	Thermal constant, Band 10	774.89
K_2		1321.08
O_i	Correction, Band 10	0.29

3.3. Step 3:

Normalized Difference Vegetation Index (NDVI) is essential to recognize different land cover types of the study area. NDVI value ranges between -1.0 to +1.0. NDVI is calculated using the formula given below.

$$NDVI = \frac{(NIR - RED)}{(NIR + RED)} \quad (3)$$

Where NIR represents the near-infrared band (Band 5: 0.85-0.88μm) and *R* represents the red band (Band 4: 0.64 - 0.67μm). Calculation of NDVI is necessary to further calculate proportional vegetation (P_v) and emissivity (ε) (Weng, Lu, & Schubring, 2004).

3.4. Step 4:

Next step is to calculate proportion of vegetation (P_v) from NDVI values received in step 3. The bare soil and vegetation proportions are acquired from the NDVI of pure pixels. Values of NDVIs = 0.2 and NDVIv = 0.5 had been proposed to apply in global conditions. While the value for vegetated surfaces (NDVIv = 0.5) may be too low in some cases Global values from NDVI can be calculated at-surface reflectivity, but it would not be possible to establish global values in the case of an NDVI computed from TOA reflectivity, since $NDVI_V$ and $NDVI_s$ will rely on the atmospheric conditions.

$$P_V = \left(\frac{NDVI - NDVIs}{NDVIv + NDVIs}\right)^2 \quad (4)$$

3.5. Step 5:

The land surface emissivity **(LSE (ε))** must be known so as to evaluate LST, since the LSE is a proportionality factor that scales blackbody radiance (Planck's law) to expect emitted radiance, and it is the proficiency of transmitting thermal energy across the surface into the climate (Yadav, Singh, Jadaun, kumar, & Upadhyay, 2019).

$$\varepsilon_\lambda = \varepsilon_{v\lambda} P_v + \varepsilon_{s\lambda} (1 - P_v) + C_\lambda \quad (5)$$

where εV and εs are the vegetation and soil emissivity, and C represents the surface roughness (C= 0 for homogenous and flat surfaces) taken as a constant value of 0.005(Raissouni & Sobrino, January 2000).When the **NDVI** is less than 0, it is classified as water, and the emissivity value of **0.991** is assigned. For NDVI values between **0 and 0.2**, it is considered that the land is covered with soil, and the emissivity value of **0.996** is assigned. Values between **0.2 and 0.5** are considered mixtures of soil and vegetation cover. In the last case, when the NDVI value is greater than **0.5**, it is considered to be covered with vegetation, and the value of **0.973** is assigned (Yadav, Singh, Jadaun, kumar, & Upadhyay, 2019).

3.6. Step 6:

The last step of retrieving the **LST** or the emissivity corrected land surface temperature ***Ts*** is computed as follows;

$$Ts = \frac{BT}{\{1 + [(\lambda BT/\rho) \ln \varepsilon\lambda]\}} \quad (6)$$

Where:
Ts = LST in Celsius (°C)
BT =brightness temperature (°C),
λ = wavelength of emitted radiance (for which the peak response and the average of the limiting wavelength (λ =10.895) will be used),
$\varepsilon\lambda$ = emissivity calculated

$\rho = hc\sigma = 1.438 \times 10^{-2}$mK,
Where σ is the Boltzmann constant (1.38×10^{-23} J/K), h is Planck's constant (6.626×10^{-34} J s), and c is the velocity of light (2.998×10^{8} m/s) (Yadav, Singh, Jadaun, kumar, & Upadhyay, 2019)

4. RESULT

4.1. Change in urban sprawl from 2014 to 2018

By using the urban sprawl map of year 2014 and 2018, it can be easily estimate that there is increase in the urban sprawl from 2014 to 2018, by subtracting the urban sprawl area of 2014 from the urban sprawl area of 2018 which is given in the figure no 3 and the total area in following formula;

= Urban Sprawl of 2018 - Urban Sprawl of 2014

= (372.1428 - 346.119) km^2

= 26.023km^2

The increased area in urban sprawl from 2014 to 2018 is approximately 26.023 km^2, which is due to increase in population, mitigation, and urbanization.

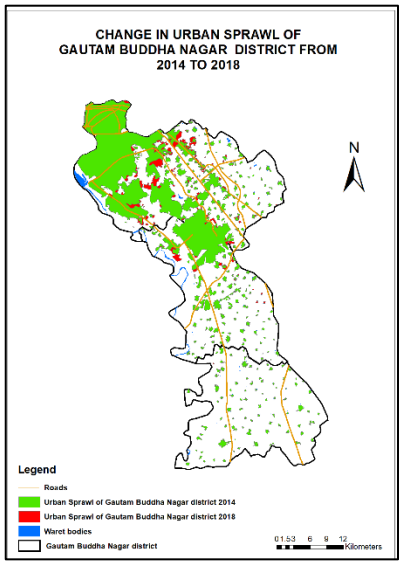

FIGURE 3: change in urban sprawl of Gautam Buddha Nagar district from 2014 to 2018

4.2. Change in Land Surface Temperature (LST) from 2014 to 2018

The maps given in figure no 4 (for march months) and table (3 and 4) demonstrate the continuous increase in urban sprawl results increase of land surface temperature from 2014 to 2018 over Gautam Buddha Nagar district of Uttar Pradesh, India and the other maps for different months are given in the figure no. 5 and 6. The result shows that densely urban built-up lands were in the central part of this study area and high LST values are obtained with maximum population density in this part as well as due to increasing urban area the temperature in the central and outskirts are also increasing. By using this information we can find the hot spot areas to minimized the effect of the rise of temperature and control the over pollutions.

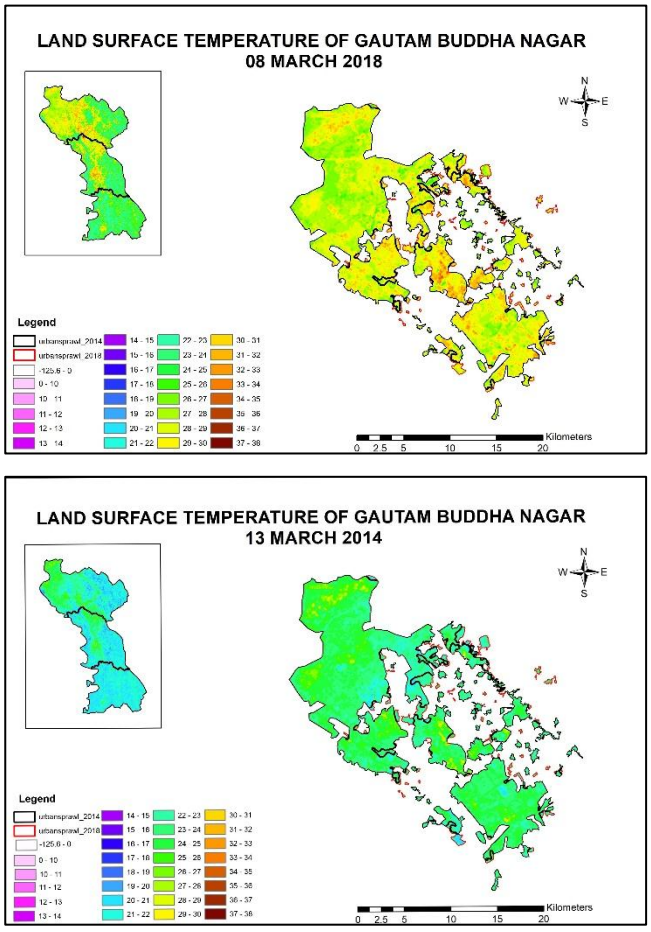

FIGURE 4: change in land surface temperature of Gautam Buddha Nagar district from 2014 to 2018

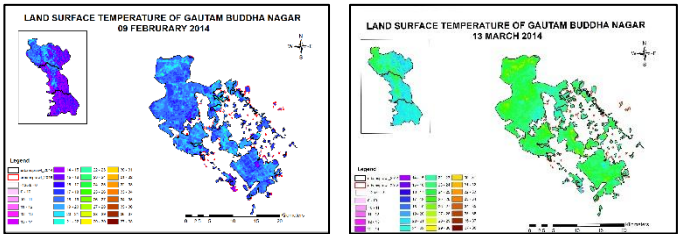

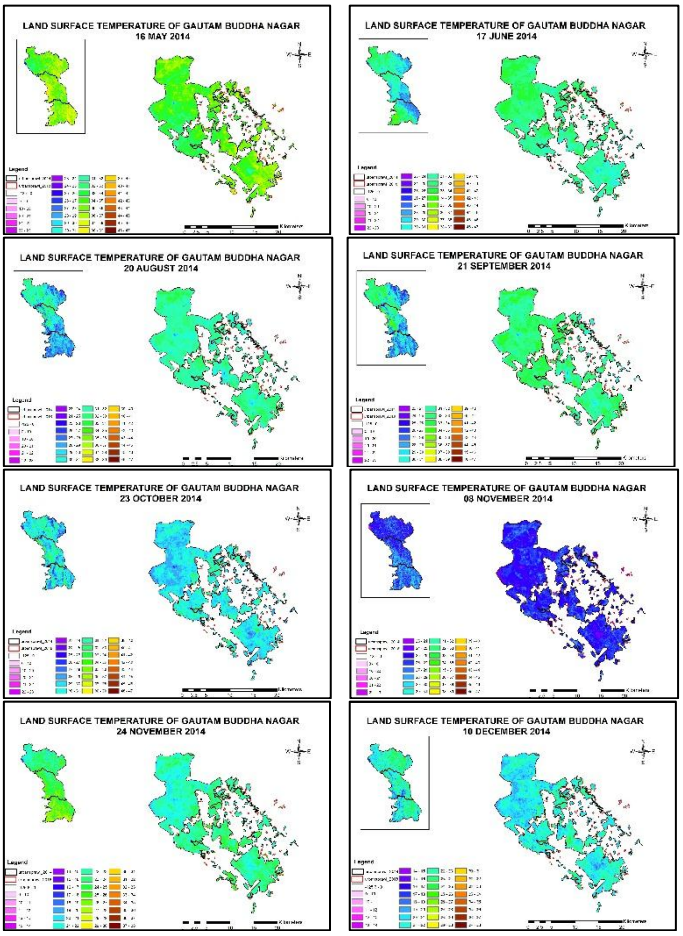

FIGURE 5: land surface temperature of (lst) Gautam Buddha Nagar district 2014

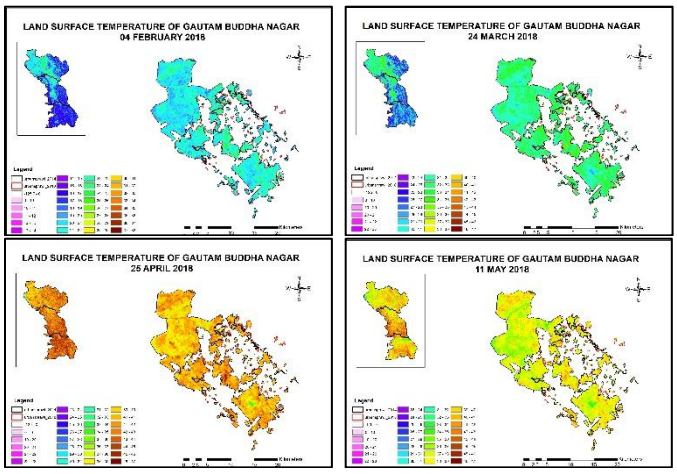

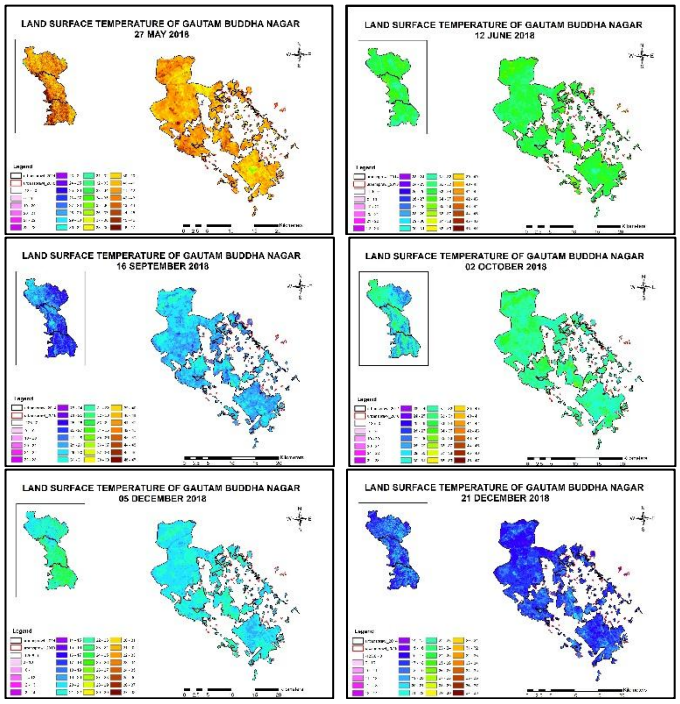

FIGURE 6: land surface temperature of (LST) Gautam Buddha Nagar district 2018

4.3. Comparison of monthly land surface temperature

Land surface temperature from 2014 and 2018 were estimated monthly with Landsat 8 satellite. Landsat 8 satellite provide 16 days temporal resolution data. With the help of grid indexing feature in ArcGIS 1 X 1 grid was made and centroidal points were marked to estimate the temperature as shown in figure 7. The temperature of different month of 2014 and 2018 over Gautam Buddha Nagar is shown in table no. 3 and 4. The Comparison of average monthly LST of 2014 and 2018 over Gautam Buddha Nagar is shown in figure 8.

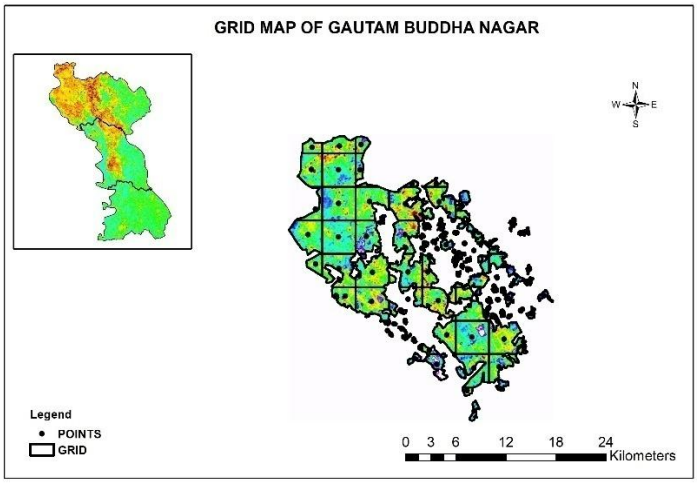

FIGURE 7: grid map of Gautam Buddha Nagar district

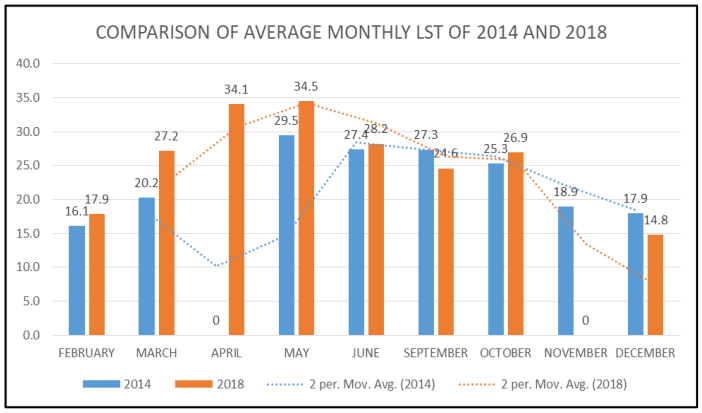

FIGURE 8: comparison of average monthly land surface temperature of 2014 and 2018

TABLE 3: land surface temperature of different point for 2014

SN.			2014							
1	POINT_X	POINT_Y	FEB	MARCH	MAY	JUNE	SEPT	OCT	NOV	DEC
2	77.329901	28.675338	20.3	26.6	37.1	33.6	34.1	30.8	23.4	21.8
3	77.36357	28.676317	18.9	25.2	35.9	32.5	32.9	30.2	22.6	21.2
4	77.390433	28.677325	18.8	25.0	35.1	32.7	32.7	29.6	22.7	21.2
5	77.328782	28.651621	23.7	29.1	37.3	34.7	35.0	32.6	25.1	24.1
6	77.362031	28.650505	18.1	22.8	31.5	30.7	30.4	28.8	20.6	19.7
7	77.388296	28.650149	18.7	22.8	33.5	31.3	31.7	29.1	22.0	21.1
8	77.451594	28.633459	21.8	24.3	37.2	34.4	33.7	31.0	23.3	22.6
9	77.481489	28.63312	0.0	0.0	0.0	0.0	0.0	0.0	0.0	0.0
10	77.332796	28.608812	0.0	0.0	0.0	0.0	0.0	0.0	0.0	0.0
11	77.361229	28.614425	20.3	25.2	36.0	34.2	33.9	30.9	23.2	22.3
12	77.399167	28.615719	18.1	23.7	34.9	32.5	32.3	29.2	21.3	20.0
13	77.414254	28.597859	18.0	22.2	34.1	31.1	31.9	29.7	22.7	21.3
14	77.443149	28.612496	17.8	21.3	34.3	31.5	32.3	29.6	20.9	18.7
15	77.484617	28.613765	19.2	22.6	34.4	32.1	31.5	30.6	22.8	21.7
16	77.486047	28.594235	16.9	21.5	33.6	32.1	30.7	29.9	22.5	21.0
17	77.51286	28.608933	0.0	0.0	0.0	0.0	0.0	0.0	0.0	0.0
18	77.575565	28.593107	16.7	21.5	35.2	29.6	29.1	29.3	22.0	21.7
19	77.322996	28.581214	19.7	26.2	35.3	34.0	34.1	30.4	22.5	21.7
20	77.360422	28.57835	18.7	24.6	34.4	33.0	33.0	29.4	21.9	20.7

TABLE 4: Land surface temperature of different point for 2018

			2018							
1	POINT_X	POINT_Y	FEB	MAR	APR	MAY	JUNE	SEPT	OCT	DEC
2	77.329901	28.675338	22.2	33.7	42.4	42.5	35	30.6	33.3	17.9
3	77.36357	28.676317	21.0	32.8	41.3	41.4	34	29.7	32.6	17.8
4	77.390433	28.677325	21.0	32.8	40.8	40.7	34	29.6	31.9	17.0
5	77.328782	28.651621	24.9	35.5	43.1	44.5	36	32.2	36.7	20.1
6	77.362031	28.650505	19.8	30.2	36.6	37.7	32	28.8	31.4	16.1
7	77.388296	28.650149	20.6	31.1	38.6	39.7	32	28.7	31.3	17.1
8	77.451594	28.633459	23.6	34.0	42.5	42.9	35	29.1	32.4	18.2
9	77.481489	28.63312	0.0	0.0	0.0	0.0	0	0.0	0.0	0.0
10	77.332796	28.608812	0.0	0.0	0.0	0.0	0	0.0	0.0	0.0
11	77.361229	28.614425	22.1	33.6	42.0	43.2	35	29.2	32.5	18.3
12	77.399167	28.615719	20.6	31.8	39.6	39.8	33	30.0	32.6	16.6
13	77.414254	28.597859	21.1	32.2	39.4	39.2	32	28.7	31.6	17.6
14	77.443149	28.612496	18.5	30.8	39.4	40.1	33	28.5	30.0	15.7
15	77.484617	28.613765	21.8	31.5	39.3	39.5	33	28.5	30.6	17.2
16	77.486047	28.594235	20.7	31.1	40.9	40.1	32	26.8	29.2	17.6
17	77.51286	28.608933	0.0	0.0	0.0	0.0	0	0.0	0.0	0.0
18	77.575565	28.593107	20.0	30.0	41.0	40.6	33	27.1	29.1	17.4
19	77.322996	28.581214	21.6	32.6	41.0	41.3	33	30.3	33.9	18.4
20	77.360422	28.57835	20.5	32.2	40.0	41.9	33	29.2	32.6	17.5

5. CONCLUSION

In this paper, Landsat-8 OLI and TIRS data were used to investigate the Urban Heat Island intensity effect in Gautam Buddha Nagar Uttar Pradesh, India and to interpret the dynamic relationship between LST with urban sprawl. Urban Heat Island zones were identified through LST which were distributed along the central region extends from north-west to south-east portions of Gautam Buddha Nagar while it develops throughout the eastern part of Gautam Buddha Nagar. Bare land and built-up area are mostly responsible for LST generation. The calculated LST values reflect the effects of urban growth on study area. An increase in surface temperature is due to industrial growth, different types of economic activities, settlement, reduction of flora covers and unexpected climatic changes. This work has ultimately served as an eye-opener to some hidden facts about the hazardous impact of urbanization on LST. Present study will give an optimistic approach for future and will support progressive applications.

6. ACKNOWLEDGMENT

The authors are thankful to the Director RSAC UP, Head School of Geoinformatics (Dr. Sudhakar Shukla) and the staff of Agriculture Resources Division of RSAC Uttar Pradesh.

7. REFFRENCES

[1] Liu , L., & Zhang, Y. (2011). Urban Heat Island Analysis Using the Landsat TM Data and ASTER Data: A Case Study in Hong Kong. Remote Sensing , 1535-1552.

[2] Avdan, U., & Jovanovska, G. (2016). Algorithm for Automated Mapping of Land Surface Temperature. Hindawi Publishing Corporation , 8.

[3] Bendib, A. D. (2017). Contribution of Landsat 8 data for the estimation of land surface temperature in Batna city, Eastern Algeria. Geocarto International , 503–513.

[4] Bonafoni, S. A. (2016). Downscaling Landsat land surface temperature over the urban area of Florence. European Journal of Remote Sensing , 553–569.

[5] Bonafoni, S., & Keeratikasikorn, C. (2018). Land Surface Temperature and Urban Density: Multiyear Modeling and Relationship Analysis Using. MDPI , 1471.

[6] Carlson, T. &. (1997). On the relation between NDVI, fractional vegetation cover, and leaf area index. Remote Sensing of Environment , 241–252.

[7] Chen, Y. W. (2002). A study on urban thermal field in summer based on satellite remote sensing. Remote Sensing for Land Management and Planning , 55–59.

[8] Jeevalakshmi, D., Reddy, S. N., & Manikiam, B. (2017). Land Surface Temperature Retrieval from LANDSAT data using Emissivity Estimation. International Journal of Applied Engineering Research ISSN , 0973-4562.

[9] Jimenez-Munoz, J., Sobrino, J., Gillespie, A., Sabol , D., & Gustafson, W. (2006). Improved land surface emissivities over agricultural. Remote Sensing of Environment , 474–487.

[10] Jimenez-Munoz, J.-C., Sobrino, J., Skokovic, D., Mattar, C., & Cristóbal Rosselló, J. (2014). Land Surface Temperature Retrieval Methods From Landsat-8 Thermal Infrared Sensor Data. Geoscience and Remote Sensing Letters, IEEE , 1840- 1843.

[11] Joshi, J. P., & Bhatt, B. (2012). ESTIMATING TEMPORAL LAND SURFACE TEMPERATURE USING. International Journal of Applied Engineering Research ISSN , 2277-2081.

[12] Raissouni, N., & Sobrino, J. (January 2000). Toward Remote Sensing Methods for Land Cover Dynamic Monitoring: Application to Morocco. International Journal of Remote Sensing , 353-366.

[13] Tomlinson, C., Chapman, L., Thornes, J. E., & Baker, C. (2011). Remote Sensing Land Surface Temperature for Meteorology and Climatology: A Review. METEOROLOGICAL APPLICATIONS , 296–306.

[14] Weng, Q., Lu, D., & Schubring, J. (2004). Estimation of land surface temperature–vegetation abundance relationshipfor urban heat island studies. Remote Sensing of Environment , 467–483.

[15] Yadav, S. k., Singh, P., Jadaun, S. P., kumar, N., & Upadhyay, R. (2019). SOIL MOISTURE ANALYSIS OF LALITPUR DISTRICT UTTAR PRADESH INDIA USING LANDSAT AND SENTINEL DATA. ISPRS - International Archives of the Photogrammetry, Remote Sensing and Spatial Information Sciences .